

N84 27290

IMPROVED RESOLUTION RAIN MEASUREMENTS
FROM SPACEBORNE RADAR ALTIMETERS

Julius Goldhirsh and Frank Monaldo
The Johns Hopkins University
Applied Physics Laboratory
Johns Hopkins Road
Laurel, Maryland 20707

ABSTRACT

It is demonstrated that improved resolution measurements of precipitation may be obtained from satellite borne radars with antenna beams having relatively large surface footprints. The method employs deconvolution and Fourier transform procedures, and assumes a knowledge of the antenna beam pattern. As an example, the technique is specifically directed towards the application of future spaceborne radar altimeters which may contain additional range gates to enable the measurement of rain at altitude. It is demonstrated that because of the natural variability of rain in the lateral extent, the standard beam averaging over the footprint could easily produce erroneous interpretations of the intensity of rain and its extent. On the other hand, many of these ambiguities may be removed employing the deconvolution techniques described.

Rain measurement of the type described here are considered vital from the standpoint of representing a flag for altimeter data that may be corrupted by rain. It also provides sorely needed rain data over the oceans where little or no such data is available.

1. INTRODUCTION

It has been pointed out that rain may distort and/or attenuate the sea surface echo returns of signals originating from spaceborne radar altimeters, resulting in gross errors of the mean sea height (Walsh, et al., 1983). The employment of a "piggyback" modification to future spaceborne altimeter systems has been suggested for measuring or monitoring the presence of rain at altitude (Goldhirsh and Walsh, 1982). The experimenter may employ this rain information as a flag for culling out the concomitant ocean surface measurements, as well as to provide additional meteorological information regarding the characteristics of precipitation.

A difficulty that is encountered in the measurement of precipitation with satellite borne, range gated radars deals with the poor resolution encountered because of the large beamwidth associated with the radar antenna located at relatively large distances from the earth. For example, the 3 dB down points for the one way antenna gain function corresponding to the Seasat altimeter antenna (1.6 degree beamwidth) located at an altitude of 800 km, gave rise to a 22.3 km diameter footprint at the earth's surface. Rain is, in general, highly variable along the horizontal extent, especially for convective types of precipitation (e.g., thunderstorms). Even

for stratiform rains (e.g., widespread precipitation), it is common for imbedded or convective cells of more intense rain rates to exist (Goldhirsh, 1983). As the return echo signal from a precipitating medium represents the convolution of the square of the gain and the true rain reflectivity profile (as will be demonstrated in Section 2), the rain reflectivity deduced from the beam averaged echo signal may be significantly smaller than the true reflectivity level. Furthermore, as the antenna sweeps by the rain structure on the ground, the inevitable beam averaging may smooth out the highly variable rain structure such as to give a distorted picture of the ground rain intensity profile.

2. FORMULATION OF THE PROBLEM

Consider the configuration depicting a satellite at an altitude, R_0 , above the mean sea surface. The satellite is assumed to have a pulsed radar having a downward pointing antenna with a beamwidth, θ_0 . We shall examine here the backscatter from the precipitation contained within a pulse volume centered at a range R .

The echo power is primarily due to backscatter from an array of raindrops within a pulse volume defined by the beamwidth and the range resolution of the pulse.

This echo power may be shown to be given by (Goldhirsh and Monaldo, 1983),

$$P_r = C_0 \cdot Z_c \quad (1)$$

where

$$Z_c(x_0) = \left(\frac{8 \ln 2}{\pi x_1 y_1} \right) \iint Z_{eq}(x, y) \exp \left\{ - (8 \ln 2) \left[\left(\frac{x - x_0(t)}{x_1} \right)^2 + \left(\frac{y}{y_1} \right)^2 \right] \right\} dx dy \quad (2)$$

$$\text{where, } C_0 = \left[\left(\frac{c \pi^3 |K_0|^2}{1024 \ln 2} \right) T G_0^2 \theta_1 \phi_1 F(B) L_T L_R \frac{P_T}{R^2 \lambda^2} \right] \quad (3)$$

where $|K_0|^2 = |(m^2 - 1)/(m^2 + 2)|$ and where the quantity $Z_c(x_0)$ is referred to as the effective beam averaged radar reflectivity factor where C_0 is an effective constant. Also, m is the complex reflective index of water drops, c is the velocity of light (m/sec), T is the pulse width (sec), P_T is the transmitted power (watts), λ is the wavelength (meters), L_T, L_R is the transmitter and receiver losses, respectively (< 1), R is the range from the radar to the center of the pulse volume, x_1, y_1 are the footprint lengths along the principal planes of the gain function, x_0 is the displacement of the beam nadir along the x direction in units of meters from a fixed origin at the ground and x, y is the planar dimensions relative to a fixed origin.

In the derivation of (2) we have integrated over the range resolution in the range direction given by $\delta = (cT/2) \cdot F(B)$, where $F(B)$ is an effective loss factor due to an assumed Gaussian filter response at the receiver (Doviak and Zrnica, 1979). For a matched filter linear receiver, $F(B) = -2.3$ dB. As a representative beam structure, we have assumed in the derivation of (2) the Probert-Jones

(1962) form of the one way gain function; namely a Gaussian structure.

$Z_{eq}(x,y)$ is the effective radar reflectivity factor for rain defined by,

$$Z_{eq} = \left(\frac{\lambda^4}{\pi^5 |K_o|^2} \right) \int_D \sigma(D) N(D) dD \quad (m^3) \quad (4)$$

where, $\sigma(D)$ is the backscatter cross section for a drop of diameter, D and $N(D)dD$ is the number of drops between the sizes of D and $D+dD$ per unit volume.

It is also tacitly assumed that the attenuating effects due to precipitation may be ignored. This assumption becomes tenable if the pulse volume near the top of the rain region is sampled. This may create the condition such that there is a negligible path length over which the signal propagates within the sampled volume.

3. BEAM AVERAGED RADAR REFLECTIVITY FACTOR EXPRESSED AS A CONVOLUTION INTEGRAL

Assume the equivalent reflectivity factor within the integrand of (2) may be expressed by the product relationship

$$Z_{eq} = Z_1(x) Z_2(y) \quad (5)$$

Substituting (5) into (2)

$$Z_c = \left(\frac{81n2}{x_1 y_1} \right) I_y I(x_o) \quad (6)$$

where

$$I_y = \int_{-\infty}^{\infty} Z_2(y) g(y) dy \quad (7)$$

$$I(x_o) = \int_{-\infty}^{\infty} Z_1(x) g(x-x_o) dx \quad (8)$$

where

$$g(y) = \exp \left[- (81n2) \left(\frac{y}{y_1} \right)^2 \right] \quad (9)$$

$$g(x) = \exp \left[- (81n2) \left(\frac{x}{x_1} \right)^2 \right] \quad (10)$$

It is interesting to note that $I(x_o)$ as given by (8) may alternately be expressed as the convolution of the gain square function, $g(x)$, and the reflectivity factor, $Z_1(x)$, where both are taken in the x direction. Hence,

$$I(x_o) = Z_1(x) * g(x) \quad (11)$$

where the * denotes the convolution.

4. EXTRACTING THE RADAR REFLECTIVITY FACTOR PROFILE FROM THE CONVOLUTION INTEGRAL

By taking the Fourier transform of both sides of (11), and employing a fundamental property of the convolution integral, we obtain

$$I(\omega) = Z_1(\omega) G(\omega) \quad (12)$$

where

$$I(\omega) = \int_{-\infty}^{\infty} I(x_0) \exp(-j\omega x_0) dx_0 \quad (13)$$

$$Z_1(\omega) = \int_{-\infty}^{\infty} Z_1(x) \exp(-j\omega x) dx \quad (14)$$

$$G(\omega) = \int_{-\infty}^{\infty} g(x) \exp(-j\omega x) dx \quad (15)$$

where $I(\omega)$, $Z_1(\omega)$, and $G(\omega)$ are respectively the Fourier transforms of $I(x_0)$, $Z_1(x)$ and $g(x)$ are given by (13) through (15). It is apparent that by solving for $Z_1(\omega)$ in (12) and applying the inverse transform to both sides (i.e., $FT^{-1}\{\}$), the profile $Z_1(x_0)$ may be established. That is,

$$Z_1(x_0) = FT^{-1} \left\{ \frac{I(\omega)}{G(\omega)} \right\} = \frac{1}{2\pi} \int_{-\infty}^{\infty} \frac{I(\omega)}{G(\omega)} \exp[+j\omega x_0] d\omega \quad (16)$$

Equation (16) represents the general formula for extracting the reflectivity profile in the x direction, given a knowledge of the measured echo power, $P_r(x_0)$, obtained as the beam sweeps the rain profile as a function of x_0 .

Substituting (10) into (15), the Fourier transform of the gain function is given by,

$$G(\omega) = \frac{1}{2} \left[\frac{\pi x_1^2}{2 \ln 2} \right]^{1/2} \cdot \exp \left[- \frac{\omega^2 x_1^2}{32 \ln 2} \right] \quad (17)$$

Substituting (17) into (16), we obtain,

$$Z_1(x_0) = \left(\frac{2 \ln 2}{\pi^3 x_1^2} \right)^{1/2} \int_{-\infty}^{\infty} I(\omega) \exp \left[+ \frac{\omega^2 x_1^2}{32 \ln 2} + j\omega x_0 \right] d\omega \quad (18)$$

Equation (18) represents the resulting expression for the reflectivity profile, where $I(\omega)$ is the Fourier transform of $I(x_0)$ obtained through the beam averaged power measurement.

5. EXPECTED POWER LEVELS FOR A REPRESENTATIVE SATELLITE BORNE RADAR

General Case

In this Section we estimate the minimum detectable beam averaged reflectivity factor and the corresponding rain rate. As an example, we shall assume similar radar parameters as those for the Seasat radar altimeter (MacArthur, 1978). These are given as follows: $\lambda = 2.22 \times 10^{-2}$ m; $P_t = 2 \times 10^3$ watts; $T = 3.2 \times 10^{-6}$ sec; $R = 8 \times 10^5$ m; $\theta_1 = \phi_1 = 1.6^\circ$ (2.792×10^{-2} radians); $G = 40.6$ dB (1.148×10^4); $L_T = -0.9$ dB (0.813); $L_R = -1.2$ dB (0.758); $|K_0|^2 = 0.9$; $F(B) = -2.3$ dB (0.59). Substituting these parameter values into (3), the power reduces to

$$P_r \text{ (dBm)} = -140.5 + \text{dBZ} \quad (19)$$

where the reflectivity factor, Z_c is in mm^6/m^3 , P_r is in dBm, and $C_0 = 8.9 \times 10^{-15}$. Also dBZ is defined by,

$$\text{dBZ} = 10 \text{ Log}_{10} Z_c \quad (20)$$

Assuming a unity signal to noise ratio of -115 dBm (5 dB smaller than the Seasat case), and solving for dBZ, we obtain $(\text{dBZ})_{\min} = -115 + 140.5 = 25.5$. Hence, the radar is capable of detecting beam averaged reflectivity factors of 25.5 dB and larger with a signal to noise ratio of 1 or larger.

To further amplify the above example, we assume the following empirical relation relating the rain rate P_r , expressed in mm/hr, to the reflectivity factor, expressed in mm^6/m^3 ,

$$R_r = (Z_c/200)^{0.625} \quad (21)$$

This relationship is consistent with the assumption of a Marshall-Palmer drop size distribution (1948). Relating (21) and (20)

$$R_r = (3.65 \times 10^{-2}) 10^{(.0625 \cdot \text{dBZ})} \quad (22)$$

Substituting a dBZ of 25.5 into (22) results in $(R_r)_{\min} = 1.4$ mm/hr.

In summary, assuming radar parameters which are the same as the Seasat altimeter, a unity signal to noise ratio of -115 dBm results in a 25.5 beam averaged reflectivity factor which is equivalent to an estimated 1.4 mm/hr rain rate.

6. DECONVOLUTION ON AN ARBITRARY REFLECTIVITY PROFILE

In this Section we demonstrate the power of the deconvolution technique in recovering high resolution reflectivity profiles. We implement this technique employing deconvolution methods as described in Section 3 and radar data of a rain reflectivity profile acquired employing a ground based radar at Wallops Island, Virginia.

In Figure 1a (solid curve) we show, as an example, a typical measured reflectivity profile over a distance interval of 90 km. This profile was obtained with a radar operating at S band (2.8

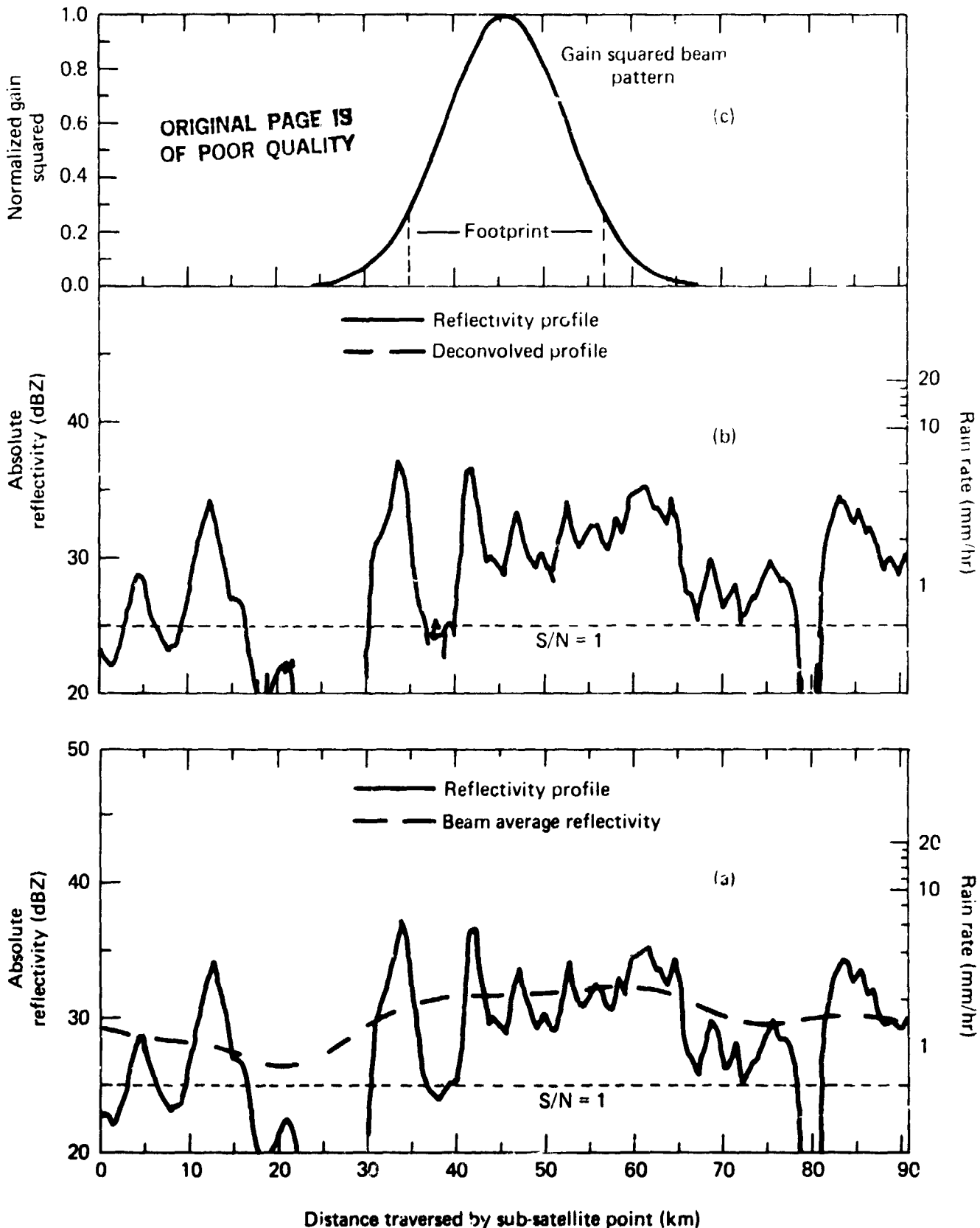


Figure 1 (a) Measured reflectivity factor profile (solid curve) and beam averaged levels (dashed curve). (b) Measured reflectivity factor profiles (solid line) and deconvolved profile (solid and dashed). (c) Gain squared beam pattern.

GHz), a low elevation angle pointing (0.5° relative to the local horizon), and a 150 m range resolution (pulsewidth = 0.5 μ sec) (Goldhirsh, 1979). The profile corresponds to the rain day January 2, 1979 and was obtained at 9:34 a.m. local time.

Shown in Figure 1-(a) is a dashed curve which represents the beam averaged reflectivity factor with values sampled every 0.7 km. This is the reflectivity that would be measured assuming the footprint of the satellite borne radar (whose parameters are given in Section 4) sweeps by the reflectivity profile. This curve was calculated by injecting the true reflectivity profile into the integral (2), where a uniform reflectivity is assumed in the cross track direction. The profile was assumed periodic in the calculation of the beam averaged values in the vicinity of the 0 and 90 km distance intervals. We note that beam averaging considerably smooths the variations of the true profile. In fact, the smoothing appears so extreme that it is difficult to visually correlate the beam averaged reflectivity with the actual profile. Also shown by the short dashed horizontal line, is the level of absolute reflectivity which would result in a unity signal to noise ratio. This corresponds to a beam averaged reflectivity factor level of approximately 25 dBZ. We note the simulated measured beam average values exceed this lower threshold level.

The right hand scale denotes the corresponding rain rate levels in mm/hr employing the empirical relationship given by,

$$R_r = 4.0 \times 10^{-3} 10^{(.086 \text{ dBZ})} \quad (23)$$

This result was calculated from drop size distribution measurements made at Wallops Island for the same rain event. We note that over the reflectivity interval, the rain rate levels are between .4 and 7 mm/hr.

In Figure 1-(c) (upper figure) is depicted the gain squared variation taken over the same abscissa scale as the actual reflectivity. It is interesting to note that considerable variation in the reflectivity profile exists over the 22.3 km footprint corresponding to the 6 dB down gain squared points.

To implement the computer simulation, the Fourier and inverse transforms were replaced by their series approximations. Specifically, the Fourier series of the gain-squared antenna pattern and the beam averaged reflectivity were computed; otherwise, the technique employed is the same as described in Section 4.

In Figure 1-(b) the dashed line represents the high resolution reflectivity data that was recovered from the beam averaged reflectivity employing the deconvolution technique. Where no dashed line is observed, the recovered level coincides with the actual reflectivity values (solid line). We note that differences are evident mostly at the very low reflectivities, equivalent to negligible rain rates, and are due to computational imprecision. This computer simulation confirms the thesis that the high resolution data can, in principle, be recovered from the beam averaged data. The above simulation was performed without injecting any contributions due to noise. The effects of noise on the resultant reflectivity profile are

examined in Section 7.

It is interesting to note that the technique is able to recover reflectivity factors at levels below the threshold noise level for the beam averaged case (i.e., below 25 dBZ). This may be attributed to the fact that the beam averaged measurement is a single measurement made by the receiver at a fixed point in space. On the other hand, the deconvolved measurement is one which employs a series of beam averaged measurements over ranges (in the example), exceeding 100 km. The effective bandwidth of the system is considerably reduced since the effective integration time is substantially increased.

7. EFFECT OF NOISE ON THE DECONVOLUTED SIGNAL

In Figure 2 we demonstrate the effect of intrinsic noise on the deconvolved signal. In Figure 2-(a) is depicted the true reflectivity profile given by the solid line and the beam averaged echo (dashed line). Superimposed on the beam averaged echo is the Rayleigh fading noise introduced by the rain itself. As an example, we assume the capability of measuring 400 independent samples. The estimate of the average power for such a case follows a Gaussian probability density distribution (Goldhirsh, 1979). A sample size of 400 hence produces a standard error of $.05\%$ (reciprocal of the square root of the sample size) or approximately 0.2 dB rms statistical uncertainty.

In Figure 2-(b) are shown deconvolved signals for two cases. The solid curve represents the deconvolved result derived from a beam averaged estimate corresponding to 400 independent samples as described in the above paragraph. As a basis of comparison, we show also the deconvolved result derived from the beam averaged estimate employing an extreme sample size of 10^4 independent samples.

8. CONCLUSIONS

We note that introducing noise to the technique seriously degrades the deconvolved result. However, in spite of this degradation, considerably more information is obtained regarding the magnitude and scale dimensions of the rain employing the convolution method than is obtained by the beam averaged case.

Although this method has been tailored for the measurement of rain employing a radar, its application to other types of satellite remote sensors should be explored.

9. ACKNOWLEDGEMENTS

This work was supported by NASA Goddard, NASA Wallops Flight Center, Wallops Island, Virginia 23337. Many thanks to Karen E. Melvin for typing this manuscript.

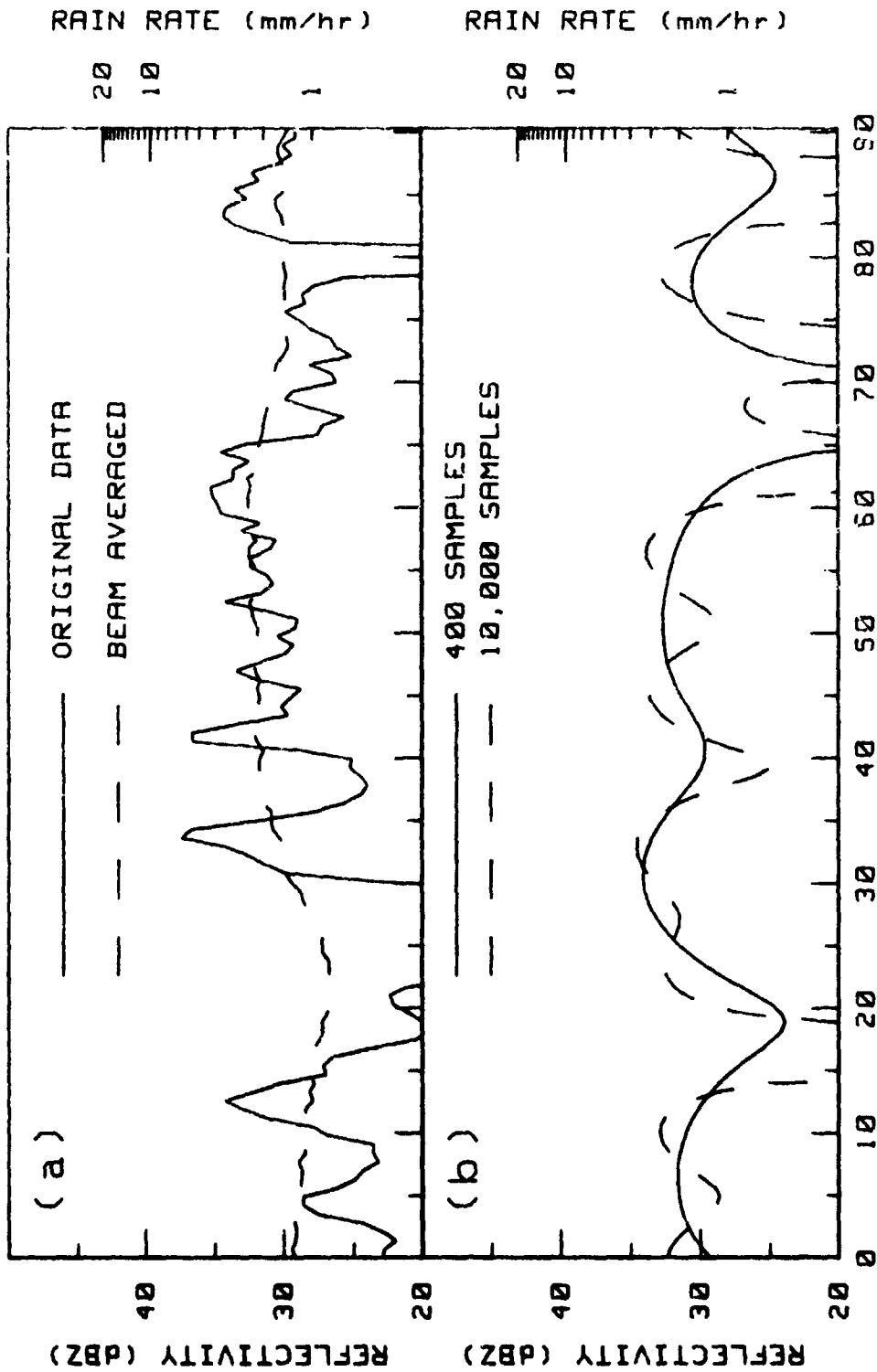


Figure 2 (a) True reflectivity factor profile (solid curve) and the corresponding beam averaged reflectivity factor with superimposed Gaussian statistical noise distribution corresponding to a sample size of 400 (dashed curve). (b) Deconvolved reflectivity factor profiles for sample sizes of 400 (solid curve) and 10,000 (dashed curve).

10. REFERENCES

- Doviak, R.J. and D. Zrnica, 1979, "Receiver Bandwidth Effects on Reflectivity and Doppler Velocity Estimates", J. of Applied Meteorology, Vol. 18, No. 1, January, pp. 70-76.
- Goldhirsh, J., 1979, "A Review on the Application of Non-attenuating Frequency Radars for Estimating Rain Attenuation and Space Diversity Performance", IEEE Transactions on Geoscience Electronics, Vol. GE-17, No. 4, October, pp. 218-239.
- Goldhirsh, J. and W.J. Walsh, 1982, "Rain Measurements from Space Using a Modified Seasat-Type Radar Altimeter", IEEE Transactions on Antennas and Propagation, Vol. AP-30, No. 4, July, pp. 726-733.
- Goldhirsh, J., 1983, "Rain Cell Size Statistics as a Function of Rain Rate for Attenuation Modeling", IEEE Transactions on Antennas and Propagation, September, Vol. AP-31, No. 5, pp. 799-801.
- Goldhirsh, J. and F. Monaldo, 1983, "Improved Resolution Rain Measurements from Spaceborne Radar Altimeters Employing Deconvolution Methods", Technical Report SLR83U-038, Applied Physics Laboratory, Johns Hopkins Road, Laurel, Maryland 20707.
- MacArthur, J.L., 1978, "Seasat-A Radar Altimeter Design Description", JHU/APL Report #SDO-5232, November.
- Marshall, J.S. and W. McK. Palmer, 1948, "The Distribution of Raindrops with Size", J. Meteor., Vol. 5, pp. 165-166.
- Probert-Jones, J.R., 1962, "The Radar Equation in Meteorology", Quarterly Journal of Royal Meteorological Society, Vol. 88, pp. 485-495.
- Walsh, E.J., F.M. Monaldo and J. Goldhirsh, 1983, "The Influence of Rain and Clouds on a Satellite Dual Frequency Altimeter System Operating at 13 and 35 GHz", Proceedings of the 1983 International Geoscience and Remote Sensing Symposium (IGARSS'83), August 31-September 2, 1983, San Francisco, California, pp. TA 5.1 - 5.10.